

Eco-Friendly Synthesis of 2,3-Dihydroquinazolin-4(1H)-ones Catalyzed by FeCl₃/Al₂O₃ and Analysis of Large ¹H NMR Diastereotopic Effect

Isabel Monreal,^a Mariano Sánchez-Castellanos,^b Karla Ramírez-Gualito,^c
Gabriel Cuevas,^d Karla A. Espinoza^a and Ignacio A. Rivero^{*a}

^aCentro de Graduados e Investigación, Instituto Tecnológico de Tijuana,
22414 Tijuana, B.C., Mexico

^bFacultad de Química de la Universidad Autónoma de México (UNAM),
Circuito Exterior s/n, Ciudad Universitaria, 04510 Mexico City, Mexico

^cInstituto de Química, Universidad Nacional Autónoma de México (UNAM),
Circuito Exterior s/n, Ciudad Universitaria, 04510 Mexico City, Mexico

^dCentro de Nanociencias y Micro y Nanotecnologías, Instituto Politécnico Nacional,
Av. Luis Enrique Erro s/n, Unidad Profesional Adolfo López Mateos, Zacatenco,
07738 Mexico City, Mexico

In the present study, we have carried out a condensation reaction for the synthesis of 2,3-dihydroquinazolin-4(1H)-ones from 2-amino-*N*-benzylbenzamide and different aromatic aldehydes using FeCl₃ catalyst supported on Al₂O₃. It was demonstrated that this material can be used successfully for the nucleation of quinazolinones with good to excellent yield; furthermore, the FeCl₃/Al₂O₃ catalyst can be recovered and reused. This catalyst was used before in the synthesis of imidazole with very good yields. The synthesized quinazolinones showed a large range diastereotopic effect over the methylene group and, this anomalous difference was studied through nuclear magnetic resonance (NMR) and computational calculations.

Keywords: quinazolinone, 2-amino-*N*-benzylbenzamide, diastereotopic, eco-friendly

Introduction

Quinazolinone (QZ) heterocycles and their derivatives are a very important group of molecules. One of the first QZ's synthesized was methaqualone (Figure 1), originally used as an antimalarian drug.¹ The sedative-hypnotic activity of methaqualone was observed since 1951; and later was used for the treatment of insomnia, as a sedative and muscle relaxant.² QZ's have a wide extent of biological actions³ such as central nervous system activity,⁴ anticonvulsant and antidepressant agents,⁵ they have been used for biological evaluation and docking studies (Alzheimer's disease),⁶ in nuclear medicine as potential labeler.⁷ Their analgesic and anti-inflammatory properties have been evaluated⁸ in endocrinology as inverse agonist for the human thyroid-stimulating hormone receptor,⁹ as enzymatic inhibitors of thermolysin¹⁰ and chorismate

mutase,¹¹ as potent antitumor agents that inhibit tubulin.¹² They have been evaluated as anticancer agents,^{13,14} for insecticidal,¹⁵ antibacterial^{16,17} and antifungal¹⁸ activity. Additionally, these compounds can easily be oxidized to their quinazolin-4(3H)-one analogs, which are biologically active compounds.¹⁹ Thus, an efficient synthesis of these compounds has been of great interest in past years.²⁰ There have been developed different methods of synthesis for 2,3-dihydroquinazolin-4(1H)-ones (DQZ) most recently; Mn^{III}-based reaction,²¹ under ultrasonic irradiation,²² zeolite catalyzed method,²³ with green chemistry using nano-indium oxide²⁴ and carbon nanotubes as a heterogeneous catalyst,²⁵ etc.²⁶⁻³¹ QZ skeleton is very common in many natural alkaloids.³²⁻³⁴ Keeping in view the above, we report a convenient and high yield eco-friendly synthesis of QZ using FeCl₃/Al₂O₃ as catalyst; FeCl₃/Al₂O₃ could be recovered and reused.

*e-mail: irivero@tectijuana.mx

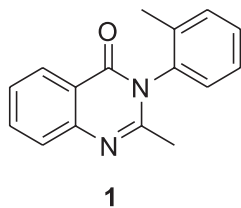


Figure 1. 2-Methyl-3-*o*-tolyl-4(3H)-quinazolinone (**1**).

Experimental

Computational methods

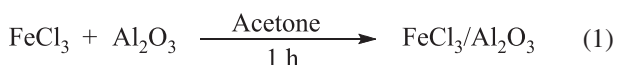
A molecular mechanics conformational analysis of compounds **3b**, **3f** and **3h** was done with the CompuVOA³⁵ commercial software. The most stable conformers were optimized at the mPW1B95/6-311+G(2d,p) level of theory with Gaussian 09.³⁶ The charge and electronic delocalization index were calculated with the wave function obtained from the optimization using the AIMAll software.³⁷

General procedures

Thin-layer chromatography (TLC) was performed on silica gel F₂₅₄ plates (Merck). All compounds were detected using UV light. Melting points were obtained on an Electrothermal 88629 apparatus and are not corrected. Infrared spectra (IR) were recorded on a PerkinElmer FT-IR 1600 spectrometer. ¹H and ¹³C nuclear magnetic resonance (NMR) spectra at 200 and 50 MHz, respectively, were recorded on a Varian Mercury 200 MHz Spectrometer in CDCl₃ and/or dimethyl sulfoxide (DMSO-*d*₆) with tetramethylsilane (TMS) as internal standard. Mass spectra were obtained on an Agilent Technologies 5975C MS Spectrometer at 70 eV by direct insertion. Diffraction data were collected on a Smart Apex X-ray diffractometer.

General method for preparing catalyst FeCl₃/Al₂O₃

In a flask, FeCl₃ (18.6 g, 11.4 mmol), Al₂O₃ (acid alumina, 10.0 g, 98.0 mmol) were placed in acetone (17 mL) and the reaction mixture was stirred constantly for 1 h. The acetone was removed under reduced pressure, then the catalyst was dried at 120 °C for 12 h in an oven under reduced pressure (equation 1).¹⁹



General method for preparing quinazolinones (**3a-3i**)

In a vial, 2-amino-*N*-benzylbenzamide (100.0 mg, 0.450 mmol), aldehyde (0.450 mmol), MeOH (2 mL),

and FeCl₃/Al₂O₃ (160 mg) were placed. It was capped and shook for 2 h, the reaction was followed by TLC and filtered by gravity. The residues were washed with ethyl acetate, the solvent was eliminated to reduced pressure, the solid obtained was purified by chromatography column, eluted with petroleum ether and EtOAc. The recovery percentage were between 85-98%.

Results and Discussion

Synthesis of quinazolinones

The *ortho*-aminobenzamide (OAB) (**2**) is a precursor of several types of compounds with biological activity. Initially, we prepare **2** from the isatoic anhydride and benzylamine in dimethylformamide (DMF) at 60 °C, allowing the formation of CO₂.³⁸ The **2** was obtained in quantitative yield.

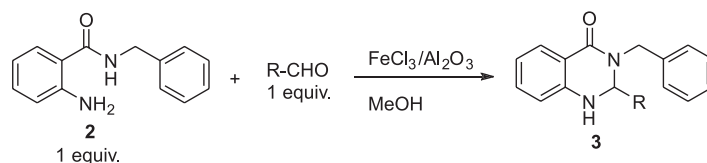
In our group, imidazole compounds were prepared with the FeCl₃/Al₂O₃ catalyst, obtaining very good yields.³⁹ This methodology was used to prepare the QZ and only produced DQZ in all cases. It was necessary to oxidize with 2,3-dichloro-5,6-dicyano-1,4-benzoquinone (DDQ) to obtain the QZ. The synthesis of DQZ was carried out with OAB and different benzaldehydes as a starting material in MeOH, using the base reaction shown on Table 1.

The catalyst was prepared with a reported methodology,⁴⁰ and the reactions were carried out at room temperature, during 4 h, to afford compounds **3a-3i** (Table 1). The nine DQZ were obtained in good to excellent yields (Table 1).

In Scheme 1, a plausible mechanism is shown that begins with the preparation of the catalyst. The FeCl₃ and the silica are mixed in an acetone solution, the solvent is removed and the FeCl₃/silica gel was dried. The FeCl₃ was adsorbed on the surface of the silica, the chloride ion occupying some vacancy of the surface causing the ferric salt to behave in ionic form. This effect of synergism due to the dissociation of the iron salt in its ionized form, increases the catalytic capacity. The Fe + salt interacts on the oxygen of the aldehyde (Scheme 1a) catalyzing the condensation of OAB to form the imine and, subsequently, this catalyst acts on the amide oxygen promoting the equilibrium with the imidic acid, which was condensed to form the imidazolinone.

¹H NMR characterization

The DQZ has a chiral center that modifies the benzyl methylene protons and makes them diastereotopic protons. These protons show a difference from 1.4 to 1.9 ppm (Table 2), which is very large and unusual, so it is an important fact to highlight (Figure 2).

Table 1. Synthesis of DQZ (**3**) from OAB (**2**)

entry	Aldehyde (1 equiv.)	Product	Yield / %	entry	Aldehyde	Product	Yield / %
1			98	6			95
2			98	7			93
3			97	8			98
4			95	9			97
5			85				

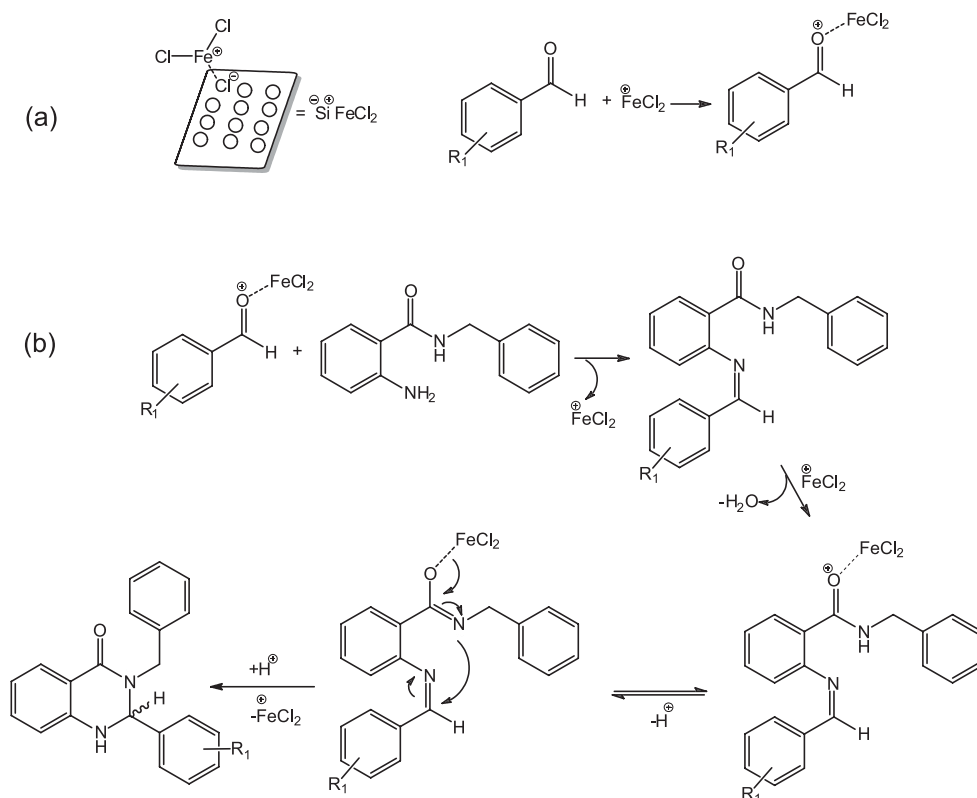
The ^1H NMR spectrum of compound **3b** shows two diastereotopic protons (proR and proS) with a chemical shift of 3.81 and 5.31 ppm, respectively. This is an unusual fact for this kind of protons and is due to the existence of a stable rotamer that makes this difference so relevant (Figure 3).

X-ray diffraction structures

In Figure 4, the ORTEP structures of compounds **3b**, **3d**, **3f**, **3g** and **3i** are shown. The bond lengths and angles related to the carbonyl group, the nitrogen bonded to this group and the methylene group that contains the two diastereotopic protons (proR and proS) were analyzed.

These molecules exhibit an unusual shift of the methylene hydrogens, which is too large for diastereotopic hydrogens. Such large differences are associated to charge transfer as is explained by computational calculation.

The geometrical properties of the molecules around the methylene group were determined by X-ray structures. Initially, the atom bonds length values were obtained: in the segment C(4)–N(3)–C(23), the C23 corresponds to the methylene carbon where the diastereotopic hydrogens are located, in **3f**, is the C25. Table 2 shows that compound **3i** has the largest chemical shift difference and has the shorter distances. The O(1)–C(4) and the N(3)–C(23) bonds distances are illustrative, it is shown that they have a very important role in the difference of the chemical shift of the diastereotopic hydrogens. When the O–C and N–C bond distances diminish, the chemical shift difference is large, with values between 1.5 and 1.9 ppm. The dihedral angle is an indication of the spatial arrangement, the negative value of the dihedral angle (O–C–N–C) affects the difference between the diastereotopic hydrogens.



Scheme 1. Mechanism proposed in the synthesis of quinazolinone **3**.

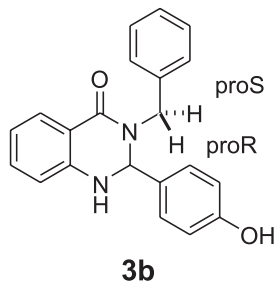


Figure 2. Diastereotopic protons in benzyl methylene of the DQZ.

Computational analysis

In order to explain the chemical shifts determined for the protons proR and proS, a conformational analysis at the molecular mechanic's level was done with the computeVOA software. In Figure 5, a selection of the most stable conformers of compound **3b** is shown. These conformers were optimized at the mPW1B95/6-311+G(2d,p) level of theory. The most important difference between these

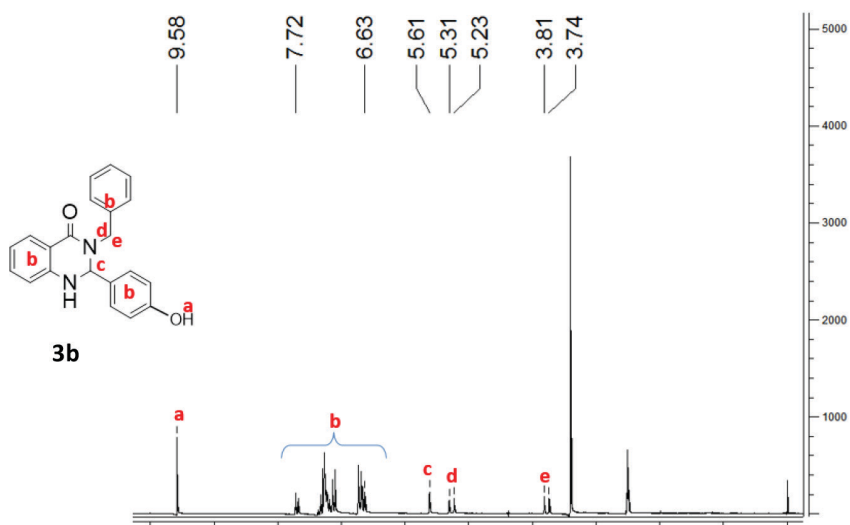


Figure 3. ¹H NMR spectrum of compound **3b** showing the differences in diastereotopic protons d and e.

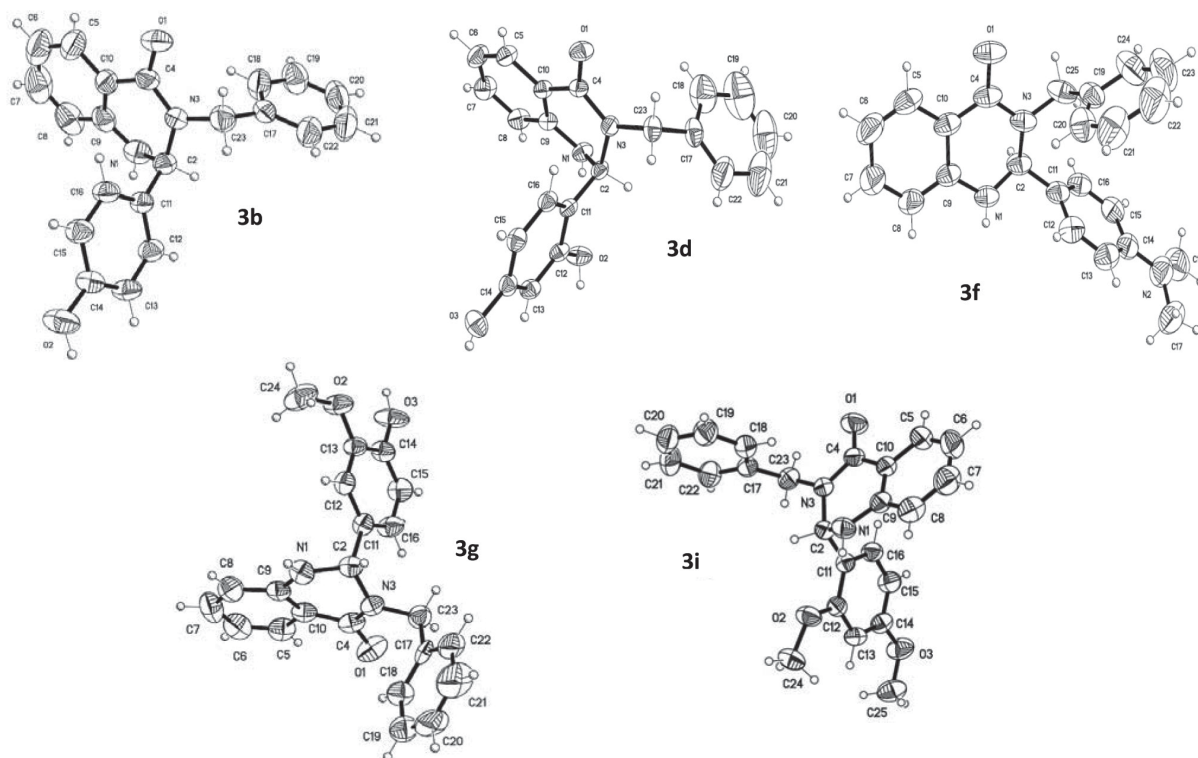
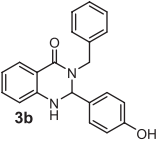
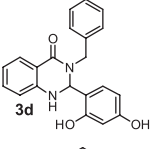
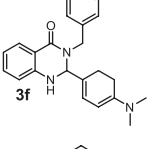
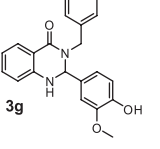
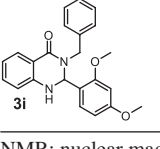


Figure 4. ORTEP structures of **3b**, **3d**, **3f**, **3g** and **3i** crystals.

Table 2. X-ray and ^1H NMR data

Structure	Bond length / Å			Dihedral angle / degree		^1H NMR δ / ppm
	O(1)–C(4)	N(3)–C(4)	N(3)–C(23)	O(1)–C(4)–N(3)–C(23)	C(4)–N(3)–C(23)–H(23e)	
	1.2478(19)	1.341(2)	1.462(2)	–3.38	135.42	1.5
	1.2546(16)	1.3466(17)	1.4705(17)	–3.24	114.26	1.5
	1.237(2)	1.362(2)	1.460(2)	–10.89	145.05	1.6
	1.259(8)	1.355(9)	1.467(8)	0.61	139.93	1.4
	1.230(18)	1.357(2)	1.452(2)	–4.57	135.63	1.9

NMR: nuclear magnetic resonance.

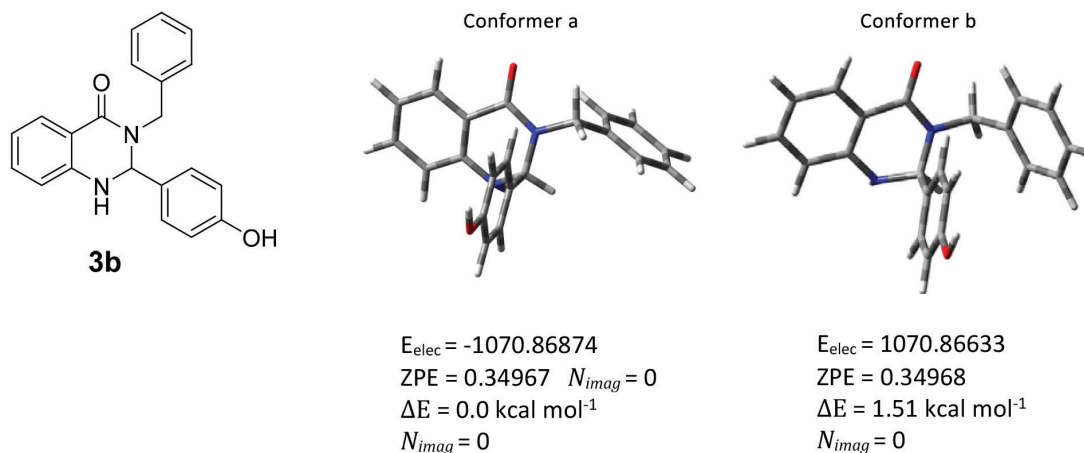


Figure 5. Lower energy conformers of compound **3b** optimized at the level of theory mPW1B95/6-311+G(2d,p). Energy values (E), zero point energy (ZPE) in Hartrees and the number of imaginary frequencies (N_{imag}) are included. $N_{imag} = 0$ refers to a structural minimum.

structures is the orientation of the hydrogen proR and proS. In conformer a, the hydrogen proR is in the same direction as the carbonyl group, while in the conformer b this occurs with the proS hydrogen.

Considering the topological theory of atoms in molecules and using the AIMAll software, the charges⁴¹ of the oxygen, hydrogens proR and proS were calculated and are summarized in Table 3.

Table 3. AIM charges of the selected conformers of **3b** calculated at the mPW1B95/6-311+G(2d,p) level of theory

Conformer	Proton		
	Oxygen	H _{proR}	H _{proS}
a	-1.187584	+0.107024	+0.027274
b	-1.190171	+0.021578	+0.086625

These results show that when the hydrogen is near to the oxygen of the carbonyl group a charge deficiency is observed. To explain the chemical shifts observed, the charge of the considered atoms was calculated considering these two conformers as in equation 2:

$$q(i) = \chi_a q(i)_a + \chi_b q(i)_b \quad (2)$$

where i represents the atom of interest, χ the conformational population of each conformer and $q(i)_x$ is the charge of i in the conformer x . Results of charges are shown in Table 4. It can be observed that the charge of the atoms is defined by the most important conformer a as expected by the energy values.

These differences in the charges can be explained by suggesting the existence of an interaction between the hydrogen proR in a and proS in conformer b with oxygen in the carbonyl group of the molecule promoting

Table 4. Charges of oxygen and hydrogens proR and proS calculated with AIM using the functional mPW1B95 and the 6-311+G(2d,p) basis

Compound	Atom		
	Oxygen	H _{proR}	H _{proS}
3b	-1.198	+0.101	+0.031
3f	-1.184	+0.104	+0.030
3h	-1.186	+0.104	+0.039

downfield shift and electronic charge deficiency generated by dispersion forces.⁴² The same analysis was done for structures **3f** and **3h**, where the same phenomenon was observed. Electronic delocalization index DI(A,B), an average number of electrons delocalized between atoms A and B, is an additional information that can be extracted from AIM calculations.⁴³ Table 5 shows the delocalization index between the oxygen and the analyzed hydrogens. These values are higher when the hydrogen is closer to the carbonyl group, showing that the difference in chemical shifts of protons proR and proS may be attributed to this interaction.

Table 5. Electron delocalization index calculated with AIM at the mPW1B95/6-311+G(2d,p) level of theory

Compound	DI(O,H _{proR})	DI(O,H _{proS})
3b	0.052525	0.007972
3f	0.054580	0.010253
3h	0.055304	0.009755

DI: delocalization index.

Conclusions

It has been shown that the use of FeCl₃/Al₂O₃ in MeOH in this reaction is an environmentally benign reaction media. This is a new approach that meet with the requirements of

sustainable chemistry. The remarkable advantages of this method are simple experiments, mild reaction conditions, excellent yields and catalyst recovery. In addition, this catalyst is highly recommended to be used in the synthesis of quinazolinones. The computational analysis of the chemical shift of the diastereotopic hydrogens indicates that the main cause of the large difference between these two hydrogens were the interaction of these hydrogens with oxygen atom. The X-ray structures show that when the distance of the C–O bond is smaller, a greater difference in ppm between the diastereotopic hydrogens is present. The dihedral angle (O–C–N–C) is another factor that affects the difference of the chemical shift of the diastereotopic hydrogens

Supplementary Information

Supplementary information (spectroscopic data, ¹H and ¹³C NMR spectra and mass spectra (EI)) is available free of charge at <http://jbc.sqbq.org.br> as PDF file.

Acknowledgments

We gratefully acknowledge the support for this project by Consejo Nacional de Ciencia y Tecnología (CONACyT, grant No. 242823) and for graduate scholarship (No. 221455), also acknowledge Tecnológico Nacional de México for support this project (Clave 5871.16-P).

References

- Kacker, I. K.; Zaheer, S. H.; *J. Indian. Chem. Soc.* **1951**, *28*, 344.
- Amin, A. H.; Mehta, D. R.; Samarth, S. S.; *Prog. Drug Res.* **1970**, *14*, 218.
- Ibrahim, S. M.; Abo-Kul, M.; Soltan, M. K.; Barakat, W.; Helal, A. S.; *Med. Chem.* **2014**, *4*, 351.
- Wolfe, J. F.; Rathman, T. L.; Sleevi, M. C.; Campbell, J. A.; Greenwood, T. D.; *J. Med. Chem.* **1990**, *33*, 161.
- Amir, M.; Ali, I.; Hassan, M. Z.; *Arch. Pharmacol. Res.* **2013**, *36*, 61.
- Liu, P.; Wang, Y. N.; Sun, Q.; Zhai, Y.; Yu, J.; Sun, J.; Xu, F.; Yan, G.; Huang, W.; Liang, L.; Xu, P.; *Eur. J. Med. Chem.* **2014**, *79*, 413.
- Kumari, S.; Kalra, N.; Mishra, P.; Chutani, K.; Mishra, A.; Chopra, M.; *Nucl. Med. Biol.* **2004**, *31*, 1087.
- El-Sabbagh, O. I.; Ibrahim, S. M.; Baraka, M. M.; Kothayeh, H.; *Archiv. Pharm.* **2010**, *343*, 274.
- Neumann, S.; Huang, W.; Eliseeva, E.; Titus, S.; Thomas, C. J.; Gershengorn, M. C.; *Endocrinology* **2010**, *151*, 3454.
- Khan, T. H.; Khan, R.; Wuxiuer, Y.; Arfan, M.; Ahmed, M.; Sylte, I.; *Bioorg. Med. Chem.* **2010**, *18*, 4317.
- Rambabu, D.; Kumar, S. K.; Sreenivas, B. Y.; Sandra, S.; Kandale, A.; Misra, P.; Basaveswara, M. V.; Pal, R. M.; *Tetrahedron Lett.* **2013**, *54*, 495.
- Chang, Y. H.; Hsu, M. H.; Wang, S. H.; Huang, L. J.; Qian, K.; Morris-Natschke, S. L.; Hamel, E.; Kuo, S. C.; Lee, K. H.; *J. Med. Chem.* **2009**, *52*, 4883.
- Rajput, S.; Gardner, C. R.; Failes, T. W.; Arndt, G. M.; Black, D. S.; Kumar, N.; *Bioorg. Med. Chem.* **2014**, *22*, 105.
- Kamal, A.; Bharathi, E. V.; Reddy, J. S.; Ramaiah, M. J.; Dastagiri, D.; Reddy, M. K.; Viswanath, A.; Reddy, T. L.; Shaik, T. B.; Pushpavalli, S. N. C. V. L.; Bhadra, M. P.; *Eur. J. Med. Chem.* **2011**, *46*, 691.
- Zhou, Y.; Feng, Q.; Di, F.; Liu, Q.; Wang, D.; Chen, Y.; Xiong, L.; Song, H.; Li, Y.; Li, Z.; *Bioorg. Med. Chem.* **2013**, *21*, 4968.
- Alaimo, R. J.; Russell, H. E.; *J. Med. Chem.* **1972**, *15*, 335.
- Mohammadi, A. A.; Askari, S.; Rohi, H.; Soorki, A. A.; *Synth. Commun.* **2014**, *44*, 457.
- Xu, Z.; Zhang, Y.; Fu, H.; Zhong, H.; Hong, K.; Zhu, W.; *Bioorg. Med. Chem. Lett.* **2011**, *13*, 4005.
- Tiwari, V. K.; Kale, R. R.; Mishra, B. B.; Singh, A.; *ARKIVOC* **2008**, *14*, 27.
- Karimi-Jaberi, Z.; Arjmandi, R.; *Monatsh. Chem.* **2011**, *142*, 631.
- Nishino, H.; Kumabe, R.; Hamada, R.; Yakut, M.; *Tetrahedron* **2014**, *70*, 1437.
- Wang, J.; Zong, Y.; Fu, R.; Niu, Y.; Yue, G.; Quan, Z.; Wang, X.; Pan, Y.; *Ultrason. Sonochem.* **2014**, *21*, 29.
- Takács, A.; Fodor, A.; Németh, J.; Hell, Z.; *Synth. Commun.* **2014**, *44*, 2269.
- Santra, S.; Rahman, M.; Roy, A.; Majee, A.; Hajra, A.; *Catal. Commun.* **2014**, *49*, 52.
- Safari, J.; Gandomi-Ravandi, S.; *RSC Adv.* **2014**, *4*, 11654.
- Sharma, M.; Pandey, S.; Chauhan, K.; Sharma, D.; Kumar, B.; Chauhan, P. M. S.; *J. Org. Chem.* **2012**, *77*, 929.
- Cabrera-Rivera, F. A.; Ortiz-Nava, C.; Román-Bravo, P.; Leyva, M. A.; Escalante, J.; *Heterocycles* **2012**, *85*, 2173.
- Zong-Bo, X.; Shi-Guo, Z.; Guo-Fang, J.; Da-Zhao, S.; Zhang-Gao, L.; *Green Chem. Lett. Rev.* **2015**, *8*, 95.
- Badolato, M.; Aillo, F.; Neamati, N.; *RSC Adv.* **2018**, *8*, 20894.
- Esmailpour, M.; Javidi, J.; Zahmatkesh, S.; Fahimi, N.; *Monatsh. Chem.* **2017**, *148*, 947.
- Hakimelahi, R.; Mousazadeh, M. H.; *Orient. J. Chem.* **2017**, *34*, 86.
- Maskey, R. P.; Shaaban, M.; Grün-Wollny, I.; Laatsch, H.; *J. Nat. Prod.* **2004**, *67*, 1131.
- Tiwary, B. K.; Pradhan, K.; Nanda, A. K.; Chakraborty, R.; *J. Chem. Biol. Ther.* **2015**, *1*, 104.
- Rajput, R.; Mishra, A. P.; *Int. J. Pharm. Pharm. Sci.* **2012**, *4*, 66.
- Debie, E.; Bultinck, P.; Nafie, L. A.; Dukor, R. K.; *ComputeVOA; BioTools*, Jupiter, FL, 2015.

36. Frisch, M. J.; Trucks, G. W.; Schlegel, H. B.; Scuseria, G. E.; Robb, M. A.; Cheeseman, J. R.; Scalmani, G.; Barone, V.; Petersson, G. A.; Nakatsuji, H.; Li, X.; Caricato, M.; Marenich, A.; Bloino, J.; Janesko, B. G.; Gomperts, R.; Mennucci, B.; Hratchian, H. P.; Ortiz, J. V.; Izmaylov, A. F.; Sonnenberg, J. L.; Williams-Young, D.; Ding, F.; Lipparini, F.; Egidi, F.; Goings, J.; Peng, B.; Petrone, A.; Henderson, T.; Ranasinghe, D.; Zakrzewski, V. G.; Gao, J.; Rega, N.; Zheng, G.; Liang, W.; Hada, M.; Ehara, M.; Toyota, K.; Fukuda, R.; Hasegawa, J.; Ishida, M.; Nakajima, T.; Honda, Y.; Kitao, O.; Nakai, H.; Vreven, T.; Throssell, K.; Montgomery Jr., J. A.; Peralta, J. E.; Ogliaro, F.; Bearpark, M.; Heyd, J. J.; Brothers, E.; Kudin, K. N.; Staroverov, V. N.; Keith, T.; Kobayashi, R.; Normand, J.; Raghavachari, K.; Rendell, A.; Burant, J. C.; Iyengar, S. S.; Tomasi, J.; Cossi, M.; Millam, J. M.; Klene, M.; Adamo, C.; Cammi, R.; Ochterski, J. W.; Martin, R. L.; Morokuma, K.; Farkas, O.; Foresman, J. B.; Fox, D. J.; *Gaussian 09, Revision A.02*; Gaussian, Inc., Wallingford, 2016.
37. Keith, T. A.; *AIMAll*, version 12.09.23; TK Gristmill Software, Overland Park, KS, USA, 2012. Available at aim.tkgristmill.com, accessed in August 2018.
38. Cortez, R.; Rivero, I. A.; Somanathan, R.; Aguirre, G.; Ramírez, F.; Hong, E.; *Synth. Commun.* **1991**, *21*, 285.
39. Monreal, I.; Torres Pacheco, L. J.; Oropeza Guzman, M. T.; Rivero, I. A.; *Int. J. Electrochem. Sci.* **2015**, *10*, 6743.
40. Chen, G. F.; Dong, X. Y.; *E-J. Chem.* **2012**, *9*, 289.
41. Bader, R.; *Atoms in Molecules: A Quantum Theory*; Oxford University Press: New York, 1994.
42. Lambert, J. B.; Mazzola, E. P.; *Nuclear Magnetic Resonance Spectroscopy: An Introduction to Principles, Applications, and Experimental Methods*; Prentice Hall: New York, 2003.
43. Buschbeck-Alvarado, M. E.; Hernandez-Fernandez, G.; Hernandez-Trujillo, J.; Cortes-Guzmán, F.; Cuevas, G.; *J. Phys. Org. Chem.* **2018**, *31*, e3793.

Submitted: May 30, 2018

Published online: August 21, 2018